

Cold Molecule Spectroscopy for Constraining the Evolution of the Fine Structure Constant

Eric R. Hudson,* H. J. Lewandowski, Brian C. Sawyer, and Jun Ye
JILA, National Institute of Standards and Technology and University of Colorado
Department of Physics, University of Colorado, Boulder, CO 80309-0440
 (Dated: October 16, 2018)

We report precise measurements of ground-state, λ -doublet microwave transitions in the hydroxyl radical molecule (OH). Utilizing slow, cold molecules produced by a Stark decelerator we have improved over the precision of the previous best measurement by twenty-five-fold for the $F' = 2 \rightarrow F = 2$ transition, yielding $(1\,667\,358\,996 \pm 4)$ Hz, and by ten-fold for the $F' = 1 \rightarrow F = 1$ transition, yielding $(1\,665\,401\,803 \pm 12)$ Hz. Comparing these laboratory frequencies to those from OH megamasers in interstellar space will allow a sensitivity of 1 ppm for $\Delta\alpha/\alpha$ over $\sim 10^{10}$ years.

PACS numbers: 33.20.Bx, 33.15.Pw, 33.55.Be, 39.10.+j

Current theories that attempt to unify gravity with the other fundamental forces predict spatial and temporal variations in the fundamental constants, including the fine structure constant, α [1]. Measurements of the variation of α by observation of multiple absorption lines from distant quasars are currently not in agreement [2, 3]. Due to the use of spatially diverse absorbers, these measurements are sensitive to relative Doppler shifts. Therefore an independent confirmation of the variation of α is important. Recently, there has been much interest in using OH megamasers in interstellar space to constrain the evolution of fundamental constants [4, 5, 6] with several important advantages. Specifically, it has been shown that the sum and difference of the $\Delta F = 0$ (F is total angular momentum) transition frequencies in the ground λ -doublet of OH depend on α as $\alpha^{0.4}$ and α^4 , respectively [4]. Thus, by comparing the values measured from OH megamasers to laboratory values it is possible to constrain α over cosmological time. Most importantly, the multiple lines (that have different dependence on α) arising from a single localized source differentiate the relative Doppler shift from the $\Delta\alpha/\alpha$ measurement. Furthermore, because of the unique properties of the λ -doublet, the $\Delta F = 0$ transitions are extremely insensitive to magnetic fields. However, as pointed out by Darling [4], for the current limits on $\Delta\alpha/\alpha$ the change in the relevant measurable quantities is on the order of 100 Hz, which prior to this work was the accuracy of the best laboratory based measurement. Thus, Darling called on the community to produce a more precise measurement of the OH λ -doublet microwave transitions to allow for tighter constraints on $\Delta\alpha/\alpha$.

Despite the prominence of the OH radical in molecular physics, the previous best measurement of the OH ground λ -doublet, performed by ter Meulen and Dymanus [7], has stood for over 30 years. This lack of improvement was due to the relatively slow progress in the center-of-mass motion control of molecules, which limited the maximum field interrogation time, and thus the spectroscopic resolution. The ability of a Stark decelerator [8, 9] to provide

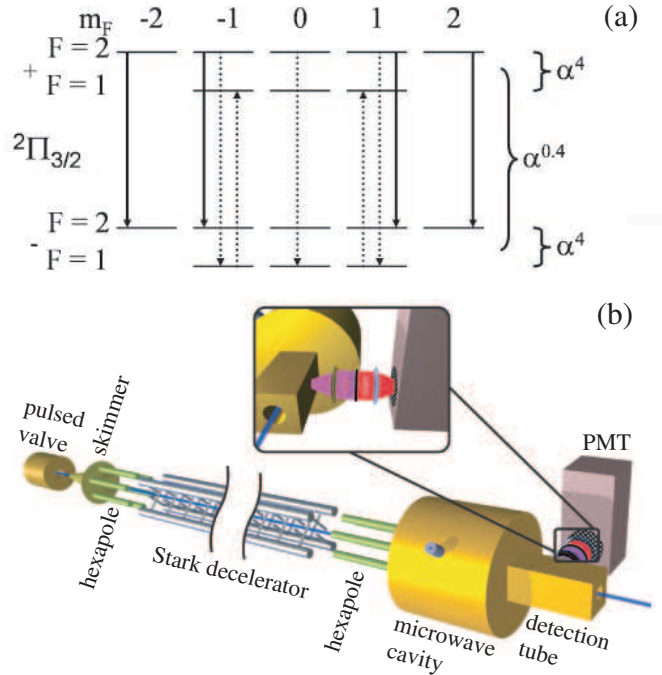


FIG. 1: (Color online) a) OH ground λ -doublet state. The arrows represent the effect of the applied microwave pulses for the $2 \rightarrow 2$ (solid arrows) and $1 \rightarrow 1$ (dotted arrows) transitions. b) Schematic of experiment (inset depicts detection region).

slow, cold pulses of molecules makes it an ideal source for molecular spectroscopy [10]. In this work, a Stark decelerator is used along with standard microwave spectroscopy techniques to perform the best measurement to date of the $\Delta F = 0$, λ -doublet microwave transitions in OH, which along with appropriate astrophysical measurements can be used to constrain $\Delta\alpha/\alpha$ with a sensitivity of 1 ppm over the last $\sim 10^{10}$ years.

In its ro-vibronic ground state OH is a Hund's case (a) molecule with a 2Π configuration and total molecule-fixed angular momentum of $\Omega = \frac{3}{2}$. For the most abundant isotopomer ($O^{16}H$) the oxygen has no nuclear

spin and the hydrogen carries a nuclear spin of $\frac{1}{2}$ leading to two total spin states with $F = 1$ and 2 . Because the unpaired electron in OH has one unit of orbital angular momentum, these ro-vibronic ground states are ‘ λ -doubled’, leading to the closely spaced opposite parity λ -doublet states shown in Fig. 1(a) labeled as $|F, m_F, \text{parity}\rangle$. Though molecules are decelerated only in the $|2, \pm 2, +\rangle$ and $|2, \pm 1, +\rangle$ states, the field-free region from the hexapole to the microwave cavity leads to an equal redistribution of the population among the five magnetic sub-levels of the $F = 2$ upper doublet state. In this work, both $\Delta F = 0$ electric dipole transitions between the upper and lower doublet states are studied. Though these transitions exhibit large Stark shifts (as is necessary for Stark deceleration), they show remarkably small Zeeman shifts. In fact, because the magnetic dipole operator respects parity, one expects the $\Delta F = 0$ transitions of a pure case (a) molecule to show no magnetic field dependence. Nonetheless, because the hyperfine splitting differs in the upper and lower doublet, and part of the $|m_F| = 1$ magnetic dipole moment comes from mixing with the other hyperfine component, there is a small quadratic shift of the $|2, \pm 1, +\rangle \rightarrow |2, \pm 1, -\rangle$ transition frequency (150 Hz/Gauss²). Furthermore, because OH is not completely case (a) (*i.e.* the electron’s orbital angular momentum and spin are slightly decoupled from the axis) the g -factor is slightly larger in the lower doublet [11]. Thus, transitions between the $m_F > 0$ ($m_F < 0$) components are blue-shifted (red-shifted) relative to the zero field value. Hence for experiments probing both positive and negative m_F components such as this work, the g -factor difference leads to a broadening and eventually a bifurcation in the lineshape for increasing magnetic field. This effect, explored at relatively large fields (0.6 - 0.9 T), was found to shift the $\Delta F = 0$ transition frequencies of the $|2, \pm 2, +\rangle$, $|2, -1, +\rangle$, and $|1, 1, +\rangle$ states at a rate of $\text{sign}(m_F) \times 2.7$ kHz/Gauss, and the $|1, -1, +\rangle$ and $|2, 1, +\rangle$ states at a rate of $\text{sign}(m_F) \times 0.9$ kHz/Gauss [11]. For even population distribution this effect leads to a shift of -450 Hz/Gauss and 900 Hz/Gauss for the $2 \rightarrow 2$ and $1 \rightarrow 1$ transitions, respectively.

Shown in Fig. 1(b) is a schematic of our experimental setup. OH molecules seeded in Xenon are created in a pulsed discharge [12] producing a molecular pulse with a mean speed of 410 m/s and 10% longitudinal velocity spread. Following a skimmer is an electrostatic hexapole used to transversely couple the molecules into our Stark decelerator, which is described in detail elsewhere [9, 13, 14]. The Stark decelerator is used in a variety of operating conditions, yielding pulses of molecules at a density of 10^6 cm⁻³ with mean speeds chosen between 410 m/s and 50 m/s with longitudinal temperatures between 1 K and 5 mK, respectively. Once the molecular pulse exits the decelerator it is focused by a second hexapole to the detection region. Located between the second hexapole and the detection region is

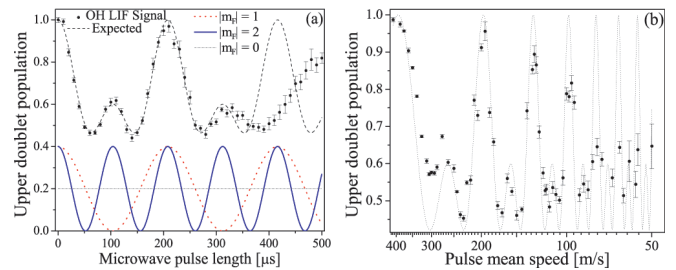


FIG. 2: (Color online) a) Rabi-flopping as a function of time. The contributions of the individual magnetic sub-levels are shown near the bottom, while the sum is shown as the dashed line. b) Rabi-flopping as a function of velocity for a fixed (spatial) length microwave pulse. The dashed line is the expected.

a 10 cm long cylindrical microwave cavity with its axis aligned to the molecular beam. The microwave cavity is operated near the TM_{010} mode, such that the electric field is extremely uniform over the region sampled by the molecules [15]. The microwave cavity is surrounded by highly magnetically permeable material to provide shielding from stray magnetic fields. From measurements of the magnetically sensitive $F = 2 \rightarrow F = 1$ transition frequency the residual field in the cavity was determined to be < 2 milliGauss. This small field results in an absolute Zeeman shift of < 0.9 Hz and < 1.8 Hz for the $2 \rightarrow 2$ and $1 \rightarrow 1$ transitions, respectively. Note that this is a cautious upper-bound on the Zeeman shift, since it is based on work performed at $\sim 10^7$ larger magnetic field where the angular momentum decoupling is enhanced. Furthermore, it was verified within experimental resolution that there were no transition frequency shifts due to stray electric fields.

Two independently switchable microwave synthesizers, both referenced to a Cesium standard, are used to provide the microwave radiation for driving the λ -doublet transitions. For probing the $|2, m_F, +\rangle \rightarrow |2, m_F, -\rangle$ λ -doublet transition ($2 \rightarrow 2$) only one synthesizer is needed since the molecules enter the cavity in the $F = 2$ state. Accordingly, two synthesizers are needed for probing the $1 \rightarrow 1$ transition. The first synthesizer transfers molecules from the $F = 2$ upper doublet state to the $F = 1$ lower doublet state. The second synthesizer then probes the $1 \rightarrow 1$ transition. After the molecules exit the cavity the population of the upper doublet is probed by laser-induced fluorescence (LIF). For the LIF measurement the molecules are excited along the $^2\Sigma_{1/2}(v = 1) \leftarrow ^2\Pi_{3/2}(v = 0)$ line at 282 nm by light produced from a doubled pulsed-dye laser. This excited state decays primarily along $^2\Sigma_{1/2}(v = 1) \rightarrow ^2\Pi_{3/2}(v = 1)$ at 313 nm. The red-shifted fluorescence is collected and imaged onto a photomultiplier tube coupled to a multi-channel scaler.

To characterize the performance of the microwave cavity the population in the upper doublet was recorded as a function of applied microwave pulse length as shown

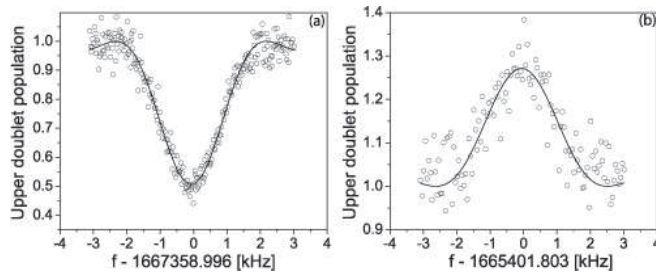


FIG. 3: Representative line shape of the 2→2 (a) and 1→1 (b) transitions. Both measurements correspond to an interaction time of 0.5 ms ($v = 200$ m/s). A center frequency is extracted from each fit (solid line).

in Fig. 2(a) (so-called Rabi-flopping). For the data shown, the molecules were decelerated to 200 m/s and a microwave pulse resonant with the 2→2 transition was applied such that its midpoint time coincided with the molecules being at the cavity center. Thus, as the pulse length was increased the molecules encountered a pulse that grew symmetrically about the cavity center. Because the LIF detection scheme is sensitive to all molecules in the upper doublet and the applied microwave field simultaneously drives transitions between the different magnetic sub-levels, the Rabi-flopping signal is more complicated than the traditional $\sin^2(\frac{\omega'_R t_p}{2})$. Here ω'_R is the effective Rabi frequency given in terms of the detuning, δ , and Rabi frequency, ω_R , as $\omega'_R = \sqrt{\delta^2 + \omega_R^2}$, and t_p is the microwave pulse length. As shown in Fig. 1(a) for the 2→2 transition (solid arrows), both the $|m_F| = 2$ and $|m_F| = 1$ magnetic sub-levels are driven by the microwave field (the $|m_F| = 0$ level has a zero transition moment). Because the electric dipole transition moment of the $|m_F| = 2$ is twice that of $|m_F| = 1$ [16], the Rabi-flopping signal exhibits beating. The calculated individual magnetic sub-level contributions are shown at the bottom of Fig. 2(a) with their sum represented by the dashed line plotted over the data. The data points were determined by comparing the populations in the upper doublet at the detection region with and without the microwave field applied. Clearly, the behavior is exactly as expected until $t_p \geq 300 \mu\text{s}$ when ω_R of both the $|m_F| = 2$ and $|m_F| = 1$ transitions appears to decrease. This reduction in ω_R is the result of the electric field diminishing near the cavity end-caps [17].

Alternatively to fixing the molecular velocity, v , and varying t_p , the Stark decelerator allows v to be varied while applying a fixed (spatial) length microwave pulse. This allows a check of systematics associated with beam velocity. Data taken in this manner is shown in Fig. 2b, where a microwave pulse resonant with the 2→2 transition was applied for the entire time the molecules were in the cavity. The microwave power for this measurement was chosen such that molecules with a 400 m/s velocity underwent one complete population oscillation

(*i.e.* a 2π pulse for the $|m_F| = 1$ and a 4π pulse for the $|m_F| = 2$ transitions). This was done so that population revivals occurred at velocities that were integer sub-multiples of 400 m/s. While the behavior agrees well with the expected (dotted line), there are two noticeable deviations. First, for $270 \text{ m/s} \leq v \leq 400 \text{ m/s}$ the fringe visibility is less than expected. This is because, as detailed in our earlier work [13, 14], molecules with these relatively high velocities have not been decelerated out of the background molecular pulse. Thus, molecules with a large distribution of speeds (as compared to the decelerated molecules) are detected, leading to reduced contrast. Second, substantial decoherence is observed for $v \leq 130$ m/s. The source of this decoherence has been experimentally determined as the result of microwave radiation leaking from the cavity and being reflected off the decelerator back into the cavity. It is interesting to note that since the metal detection tube acts as a waveguide with a cut-off frequency much higher than that applied, no radiation leaks from the rear of the cavity. Thus, future experiments should include a small waveguide section on both sides of the cavity to prevent leakage. Furthermore, because this decoherence is due to reflected radiation it is microwave power dependent, and presents no problem for the transitions frequency measurements, which use $< 10\%$ of the microwave power used in Fig. 2, such that no noticeable decoherence occurs.

Because two magnetic sub-levels with differing ω_R 's undergo the 2→2 transition, the traditional Rabi-spectroscopy method of applying a π pulse over the length of the cavity is not optimal. Thus, for measurements of the 2→2 transition frequency the microwave power was chosen such that for $\delta = 0$ the maximum contrast was produced with as small a microwave power as possible (*i.e.* transfer the molecules to the first dip in Fig. 2(a) over the length of the cavity). Representative data for the 2→2 transition is shown in Fig. 3(a) where the driving frequency, f , is varied under a fixed microwave power. Data points in this graph were generated by comparing the population in the upper doublet at the detection region with and without the probing microwave field. The fit to the data (solid line) is generated from the typical Rabi lineshape formula except contributions from the different magnetic sub-levels are included. For probing the 1→1 transition it is necessary to prepare the molecules in a $F = 1$ level since they originate in the $|2, m_F, +\rangle$ level from the Stark decelerator. This is accomplished by using the first 70 μs the molecules spend in the cavity to drive them on the satellite 2→1 line, yielding molecules in the $|1, \pm 1, -\rangle$ and $|1, 0, -\rangle$ states (downward dotted arrows in Fig. 1). The remaining time the molecules spend in the cavity (depending on v) is then used to probe the 1→1 transition frequency by applying a π pulse, which transfers only the $|m_F| = 1$ molecules to the upper doublet (upward dotted arrows in Fig. 1). Representative data for the 1→1 transition is

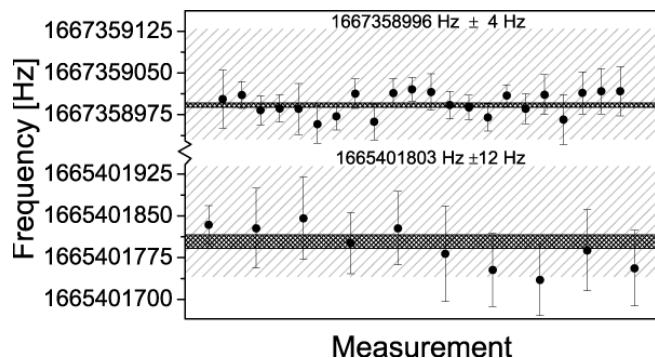


FIG. 4: Results of multiple measurements of the $2 \rightarrow 2$ transition (upper) and the $1 \rightarrow 1$ transition (lower).

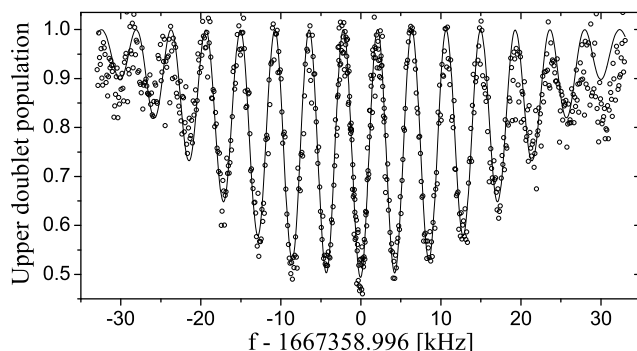


FIG. 5: Ramsey spectroscopy for the $2 \rightarrow 2$ transition with 0.2 ms pulse separation time.

shown in Fig. 3b. In contrast to the $2 \rightarrow 2$, line the LIF signal is maximum on resonance because molecules are being transferred into the detected upper doublet. Also, because only 40% of the population participate in the transitions (*i.e.* the $|m_F| = 1$) the contrast between on and off resonance is reduced relative to the $2 \rightarrow 2$ transition, leading to a slightly larger error for determining the center frequency. For both panels of Fig. 3 the molecules were decelerated to 200 m/s yielding linewidths of 2 kHz. A typical fit determines the center frequency within 20 to 50 Hz, depending on the transition. The results of several measurements of both the $2 \rightarrow 2$ and $1 \rightarrow 1$ center frequencies are displayed in Fig. 4. Each point and its error bar represents the result of a fit to a measured lineshape like those shown in Fig. 3. Using the standard error of each fit as a weight the mean and standard error of the transition frequencies are found to be $(1\,667\,358\,996 \pm 4)$ Hz and $(1\,665\,401\,803 \pm 12)$ Hz for the $2 \rightarrow 2$ and $1 \rightarrow 1$, respectively. For comparison, the lightly hatched boxes represent the bounds set on the transition frequency by the previous best measurement [7], while the limits produced by this measurement are displayed as darker cross-hatched boxes. The transition frequencies reported here are limited only by statistical uncertainties.

The Ramsey technique of separated pulses inside the

same microwave cavity was also used to measure the transition frequencies as seen in Fig. 5 with a resolution comparable to the reported Rabi measurements. However, because the molecular pulses are extremely monochromatic, minimal gain was observed in the recovered signal-to-noise ratio. This technique will of course be critical for any future molecular fountain clock. The molecular clock could enjoy reduced systematic shifts, such as the magnetic field insensitive transitions demonstrated in this work. It will be most interesting to compare an atomic clock against a molecular one which depends differently on the fine structure constant.

In summary, microwave spectroscopy was performed on slow, cold molecular pulses produced by a Stark decelerator resulting in the most precise measurement of the OH $\Delta F = 0$, λ -doublet transitions. These results along with appropriate astrophysical measurement of OH megamasers can be used to produce constraints on $\Delta\alpha/\alpha$ with a sensitivity of 1 ppm over the last $\sim 10^{10}$ yr. At the same time the use of cold molecules for the most precise molecular spectroscopy has been demonstrated. Specifically, by producing slow, cold molecular packets the Stark decelerator allows increased interrogation time, while virtually eliminating any velocity broadening.

The authors are indebted to Steven Jefferts and John L. Hall for crucial contributions. This work is supported by NSF, NIST, DOE, and the Keck Foundation.

* ehudson@jilau1.colorado.edu

- [1] K. Olive and Y. Qian, Phys. Today **57**, 40 (2004).
- [2] J. K. Webb et al., Phys. Rev. Lett. **87**, 091301 (2001).
- [3] R. Quast, D. Reimers, and S. Levshakov, Astron. Astrophys. **415**, L7 (2004).
- [4] J. Darling, Phys. Rev. Lett. **91**, 011301 (2003).
- [5] J. N. Chengalur and N. Kanekar, Phys. Rev. Lett. **91**, 241302 (2003).
- [6] N. Kanekar, J. N. Chengalur, and T. Ghosh, Phys. Rev. Lett. **93**, 051302 (2004).
- [7] J. J. ter Meulen and A. Dymanus, Astrophys. J. **172**, L21 (1971).
- [8] H. L. Bethlem, G. Berden, and G. Meijer, Phys. Rev. Lett. **83**, 1558 (1999).
- [9] J. R. Bochinski et al., Phys. Rev. Lett. **91**, 243001 (2003).
- [10] J. van Veldhoven et al., Eur. Phys. J. D **31**, 337 (2004).
- [11] H. E. Radford, Phys. Rev. **122**, 114 (1961).
- [12] H. J. Lewandowski et al., Chem. Phys. Lett. **395**, 53 (2004).
- [13] J. R. Bochinski et al., Phys. Rev. A **70**, 043410 (2004).
- [14] E. R. Hudson et al., Eur. Phys. J. D **31**, 351 (2004).
- [15] J. D. Jackson, *Classical Electrodynamics* (John Wiley and Sons, Inc., New York, 1998), 3rd ed.
- [16] A. V. Avdeenkov and J. L. Bohn, Phys. Rev. A **66**, 052718 (2002).
- [17] For the TM_{010} mode the electric field is uniform along the cavity axis. However, due to the use of multiple frequencies, we work below the TM_{010} cavity resonance leading to the observed electric field decay.